AIP ADVANCES **4**, 097128 (2014)

Temperature dependency of the emission properties from positioned In(Ga)As/GaAs quantum dots

T. Braun,[1] C. Schneider,[1] S. Maier,[1] R. Igusa,[2] S. Iwamoto,[2] A. Forchel,[1] S. Höfling,[1,a] Y. Arakawa,[2] and M. Kamp[1]
[1]*Technische Physik, Physikalisches Institut and Wilhelm Conrad Röntgen-Research Center for Complex Material Systems, Universität Würzburg, Am Hubland, D-97074, Würzburg, Germany*
[2]*University of Tokyo, 4-6-1 Komaba, Meguro-ku, Tokyo 153-8505, Japan*

(Received 11 August 2014; accepted 11 September 2014; published online 19 September 2014)

In this letter we study the influence of temperature and excitation power on the emission linewidth from site-controlled InGaAs/GaAs quantum dots grown on nanoholes defined by electron beam lithography and wet chemical etching. We identify thermal electron activation as well as direct exciton loss as the dominant intensity quenching channels. Additionally, we carefully analyze the effects of optical and acoustic phonons as well as close-by defects on the emission linewidth by means of temperature and power dependent micro-photoluminescence on single quantum dots with large pitches. [http://dx.doi.org/10.1063/1.4896284]

The optical properties of site-controlled quantum dots grown on lithographically pre-patterned substrates[1] are frequently detrimentally influenced by defect inducted linewidth broadening mechanisms. Especially for GaInAs quantum dots grown on (001) GaAs, which is the system of choice for most fundamental semiconductor quantum optical experiments,[2] spectral diffusion can severely affect the emission properties from quantum dots positioned on top of a crystal defect. However, to date the most promising technique to obtain a high degree of absolute position control over an arbitrarily large number of QDs in one processing step is the growth of quantum dots on top of etched nanopits.[1,3] Initial reports on single QD and ensemble QD properties of such QDs have outlined the problems affiliated by this technique, namely a severe single-QD linewidth broadening by defect induced spectral diffusion[3,4] and a decreasing internal quantum efficiency by nonradiative relaxation processes.[5] Careful process and sample growth optimization[6] have led to strongly improved emission characteristics of both the single[7–9] and the ensemble QD properties[9,10] with almost comparable properties to self-assembled high quality GaInAs QDs. This has led to recent applications of such positioned QDs in cavity quantum electrodynamics experiments,[6] and even the demonstration of indistinguishable photons from QDs comprising some long range ordering.[11]

We devote this report to an in-depth analysis of broadening mechanisms. The sample with a large QD pitch (2 μm on the investigated sample piece) was optimized for single QD investigations. The growth- and fabrication recipe is described in detail in Ref. 7. Shallow nanoholes were defined into epitaxially grown GaAs buffer layers by means of electron beam (E-beam) lithography and wet-chemical etching. On top of these patterned surfaces, ordered layers of site-controlled QDs were grown on a layer sequence comprising a seeding-layer and two GaAs separation layers. The growth sequence is schematically depicted in the cartoon in Fig. 1(a), whereas Fig. 1(b) shows an atomic force microscope (AFM) image of an uncapped quantum dot array with 2 μm periodicity to

[a]Present address: SUPA, school of physics and astronomy, University of St. Andrews, St. Andrews KY16 9SS, United Kingdom.

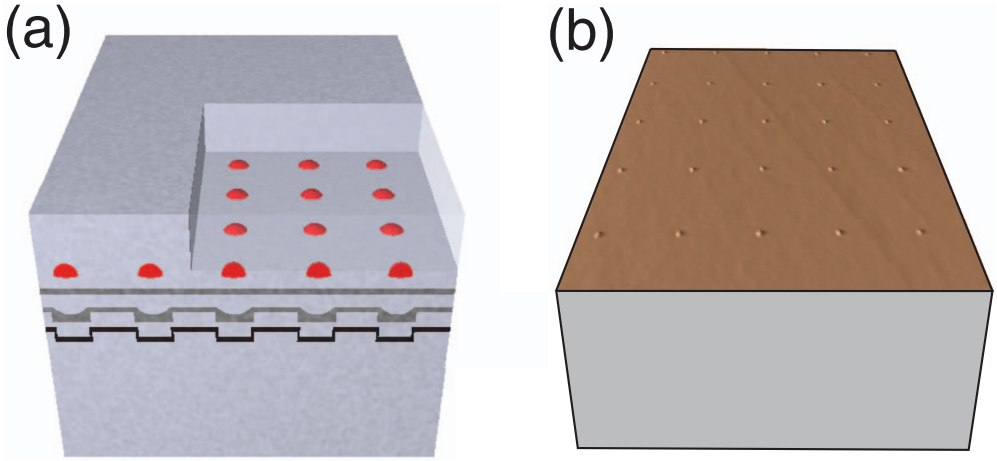

FIG. 1. (a) Cartoon of the sample growth sequence. (b) AFM image of an uncapped quantum dot array with 2 μm period on a reference sample, showing the long range ordering.

visualize the long range ordering of the QDs. Because of the large spacing only a few quantum dots are excited by the Nd:YAG-Laser emitting at a wavelength of 532 nm. A 50x microscope objective with a numerical aperture of NA = 0.42 was used to focus the beam onto the sample.

Figures 2(a) and 2(b) show emission spectra from two selected SCQDs (labeled as QD A and B in the following) from this sample at different temperatures up to 93 K. While QD A comprises a linewidth of 98.8 ± 0.9 μeV at 15K, the dominant emission feature of QD B has a linewidth of only 48.3 ± 0.8 μeV under these excitation conditions. We will only focus on the dominant emission feature in the spectrum, presumable representing the neutral exciton line. The close-by lines are attributed to multi-excitonic and charged complexes from the same QD or from emission from neighboring SCQDs which are simultaneously excited. As discussed in[7] we excluded the occurrence of the emission from interstitial QDs by highly spatially resolved scanning techniques. By increasing the sample temperature, both QDs show a redshift of their emission line, caused by the shrinking of the material bandgap. Due to thermal activation of the carriers and the rather shallow confinement the measured intensity strongly drops for higher temperatures. However the intensity of QD A drops more rapidly than for QD B. To discuss this further we take a closer look on the temperature dependence of the integrated intensity. Fig. 2(c) and 2(d) show the integrated intensity over 1/T in a semi-logarithmic plot. A simple rate equation model[12] leads to equation (1) which describes the observed behavior in good agreement:

$$I(t) = \frac{I_0}{1 + C_1 * e^{-\frac{E_1}{k_b T}} + C_2 * e^{-\frac{E_2}{k_b T}}}, \tag{1}$$

The acquired data can only be reproduced accurately over the entire temperature range by taking two different loss channels with activation energies E_1 and E_2 into account. In this model, I_0 is the extrapolated integrated QD intensity at 0 K and C_1 and C_2 describe the proportion of both loss channels. The parameters obtained by fitting the measured data are shown in the respective figure. Whereas the smaller activation energy is responsible for the initial drop in the QD intensity, and correlates with the activation from an electron trapped in the QD ground state into the surrounding barrier or delocalized states in the wettinglayer. The values determined for the two QDs are $E_{1A} = 30.7 \pm 1.1$ meV for QDA (and $E_{1B} = 17.4 \pm 1.2$ meV for QDB), which are in general agreement with calculations of InGaAs QDs with a height of ∼2 nm, a base-length of ∼25 nm and an indium content of 50 %, amounting to ∼30 meV. The deviation from this value for QDB can be explained by the shape anisotropy between different QDs, causing strong shifts in the energy levels via the effects of quantum confinement. The second term in Eq. (1) describes the behavior in the higher temperature region. Here the activation energies $E_{2A} = 102.2 \pm 0.4$ meV and $E_{2B} = 163.2 \pm 1.3$ meV

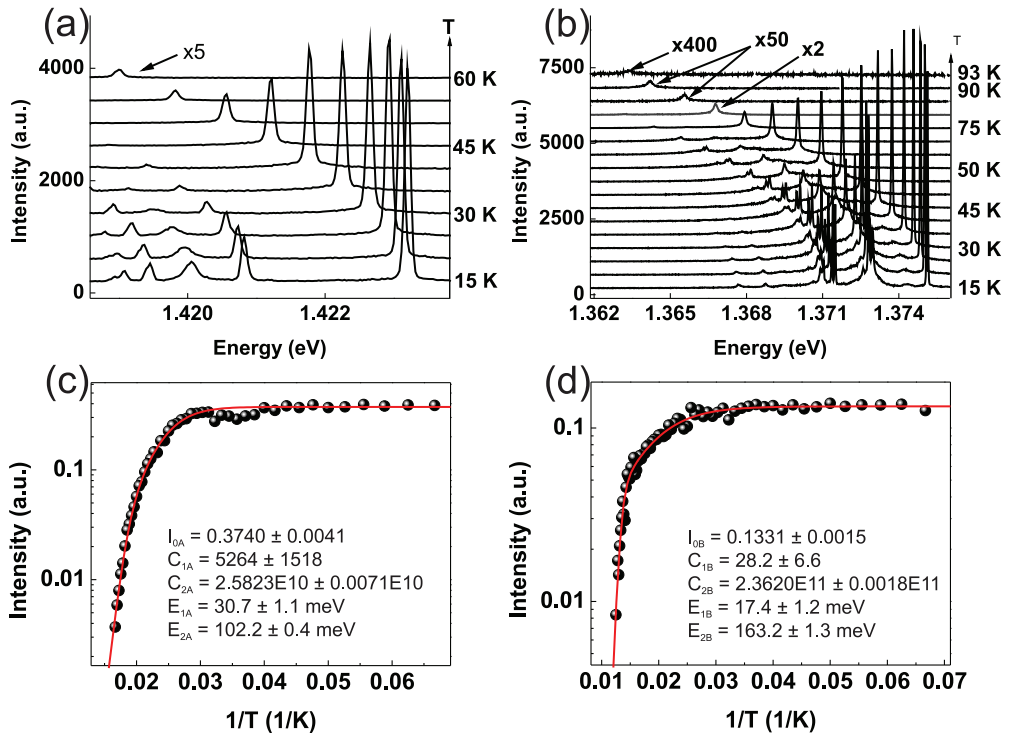

FIG. 2. (a) and (b) show temperature dependent emission spectra of QD A and QD B, respectively. (c) Integrated intensity versus 1/T in a semi-logarithmic plot for QD A and for QD B (d). The solid line gives the fit of the data by equation (1). The fit parameters are shown in the respective graphs.

are in agreement with the energetic exciton confinement in the QDs (i.e. the difference between the exciton transition energy and the GaAs bandedge) which amounts to 100 meV for QDA vs. 144 meV for QDB. This value describes the deviation in the high temperature region from a single-exponential intensity drop.

Additionally, the sample temperature also has a strong influence of the single-QD emission lineshapes, as for example discussed in Ref. 13 for high quality self-assembled QDs. In order to determine the broadening properties of our SCQDs, we investigated the temperature and power induced broadening of the lines. Fig. 3(a) and 3(b) depict the temperature dependent linewidth of QD A and QD B, respectively. The full width at half maximum (FWHM) of the single QD emission linewidth is plotted as a function of the sample temperature. The increase in linewidth attributed to acoustic and optical phonon scattering can be described by following equation:[13]

$$y(T) = \gamma_0 + \gamma_{ac} T + \frac{\gamma_{op}}{e^{(E_{LO}/kT)} - 1} \tag{2}$$

Where γ_0 is the linewidth at T = 0, the second and third term give the acoustic and optical phonon scattering and E_{LO} is the activation energy of longitudinal optical-phonons. The measured data for both, QD A and QD B can be accurately reproduced by this dependency, as shown in Fig. 3(a) and 3(b). In the low temperature regime the linear term dominates and the fit leads to $\gamma_{acA} = 0.261 \pm 0.032\ \mu$eV and $\gamma_{acB} = 0.173 \pm 0.033\ \mu$eV. This is in agreement to measured values of self-assembled InAs QDs.[14] At higher temperatures exceeding 50 K, the linewdith dependency is clearly dominated by the influence of the optical phonons, causing a pronounced broadening. For both QDs, the extracted activation energy of the optical phonons (30.9 ± 4.8 meV for QD A and 32.3 ± 0.8 meV for QD B) is in agreement with reports on self-assembled InAs QDs, which gives further evidence for phononic origin of this broadening mechanism. The extrapolated single QD linewidth of both QDs at 0K are $\gamma_{T0A} = 94.63 \pm 0.76\ \mu$eV and $\gamma_{T0B} = 45.61 \pm 0.83\ \mu$eV, respectively. These values are much higher than the homogenous linewidth and may be attributed to

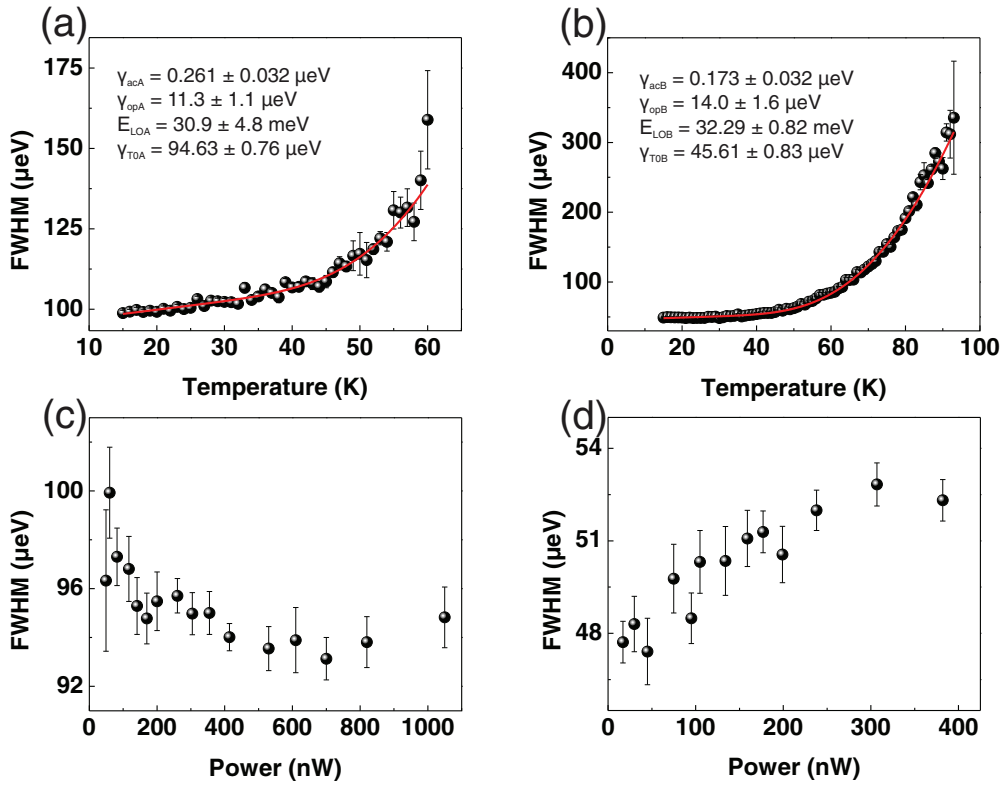

FIG. 3. (a) and (b) depict the evolution of the linewidth (FWHM) in temperature of QD A and QD B, respectively. The measured data are fitted (solid line) by equation (2) and the corresponding parameters are listed in the respective graphs. (c) Power-dependent linewidth of QD A and QD B (d).

carries that are nonresonantly generated in the QD surrounding and to defect states close by arising from the etching technique.

By studying the power dependency of the two QDs we observe a fundamentally different behavior of the emission linewidth: QD B with a higher optical quality shows the expected power broadening, which is caused by carriers in the environment of the QD (Fig. 3(d)).[15] Such power broadening phenomena have been previously reported on high quality SCQDs,[9] and high quality self-assembled QDs.[15,16] Consequently, the presence of the close-by defect is not a necessity to observe this broadening effect, however it can contribute to it. In stark contrast, the linewidth of QDA decreases with increasing power (Fig. 3(c)). We believe that this peculiarity is indeed caused by the influence of the nanopit. A large carrier reservoir excited by the excitation laser could electrostatically screen the excitons in the QD from the charges trapped in the defect, and a power induced linewidth narrowing could indeed be expected in such a configuration.

In conclusion, we have carefully analyzed the temperature dependent signatures from positioned QDs as a function of the sample temperature. Phonon related linewidth broadening was identified as the dominating broadening mechanism at sample temperatures exceeding 50 K, while spectral diffusion, which is sensitive to the excitation power, sets an inherent limit for the linewidth at lower temperatures.

ACKNOWLEDGMENTS

The authors gratefully acknowledge funding by the state of Bavaria and the bilateral project of the Deutsche Forschungsgemeinschaft (DFG) and the Japan Science and Technology Agency (JST) (project 'single quantum dot lasers'). Sample preparation by A. Huggenberger, C. Drescher and T. Steinl is acknowledged. We thank A. Musial for fruitful discussions.

[1] O. G. Schmidt, *Lateral Alignment of Epitaxial Quantum Dots* (Springer, Berlin, 2007).
[2] P. Michler, "Single Quantum Dots: Fundamentals," *Applications and New Concepts* (Springer, Berlin, 2003).
[3] C. Schneider, M. Strauß, T. Sünner, A. Huggenberger, D. Wiener, S. Reitzenstein, M. Kamp, S. Hofling, and A. Forchel, Appl. Phys. Lett. **92**, 183101 (2008).
[4] P. Atkinson, M. B. Ward, S. B. Bremner, D. Anderson, T. Farrow, G. A. C. Jones, A. J. Shields, and D. A. Ritchie, Japan. J. Appl. Phys. **45**, 2519 (2006).
[5] F. Albert, S. Stobbe, C. Schneider, T. Heindel, S. Reitzenstein, S. Höfling, P. Lodahl, L. Worschech, and A. Forchel, Appl. Phys. Lett. **96**, 151102 (2010).
[6] C. Schneider, A. Huggenberger, T. Sünner, T. Heindel, M. Strauß, S. Göpfert, P. Weinmann, S. Reitzenstein, L. Worschech, M. Kamp, S. Höfling, and A. Forchel, Nanotechnology **20**, 434012 (2009).
[7] C. Schneider, A. Huggenberger, M. Gschrey, P. Gold, S. Rodt, A. Forchel, S. Reitzenstein, S. Höfling, and M. Kamp, Phys. Stat. Sol. A 1–8 (2012).
[8] J. Skiba-Szymanska, A. Jamil, I. Farrer, M. B. Ward, C. A. Nicoll, D. J. P. Ellis, J. P. Griffiths, D. Anderson, G. A. C. Jones, D. A. Ritchie, and A. J. Shields, Nanotechnology **22**, 065302 (2011).
[9] A. Huggenberger, S. Heckelmann, C. Schneider, S. Höfling, S. Reitzenstein, L. Worschech, M. Kamp, and A. Forchel, Appl. Phys. Lett. **98**, 131104 (2011).
[10] S. Kiravittaya, A. Rastelli, and O. G. Schmidt, Appl. Phys. Lett. **88**, 043112 (2006).
[11] K. D. Jöns, P. Atkinson, M. Müller, M. Heldmaier, S. M. Ulrich, O. G. Schmidt, and P. Michler, Nano Letters **13**(1), 126–130 (2013).
[12] D. Bimberg and M. Sondergeld, Phys. Rev. B **4**, 3451 (1971).
[13] M. Bayer, G. Ortner, O. Stern, A. Kuther, A. A. Gorbunov, and A. Forchel, Phys. Rev. B **65**, 195315 (2002).
[14] C. Kammerer, G. Cassabois, C. Voisin, M. Perrin, C. Delalande, Ph. Roussignol, and J. M. Gérard, Appl. Phys. Lett. **81**, 2737 (2002).
[15] W. Bak, H. Noh, C. Stambaugh, Y. Arakawa, and W. Jhe, Appl. Phys. Lett. **100**, 022105 (2012).
[16] A. Berthelot, I. Favero, G. Cassabois, C. Voisin, C. Delalande, Ph. Roussignol, R. Ferreira, and J. M. Gérard, Nat. Phys. **2**, 759–764 (2006).